

(Research Article)**3D Modelling and Simulation Based on Kinematic Analysis for Hippotherapy****Bilal ADOUM OURADA^{*1}, Uğur FİDAN²**¹Afyon Kocatepe Üniversitesi, Fen Bilimleri Enstitüsü, Biyomedikal Mühendisliği Ana Bilim Dalı, 03030, Afyonkarahisar, ORCID No : <https://orcid.org/0000-0002-0772-3741>²Afyon Kocatepe Üniversitesi, Fen Bilimleri Enstitüsü, Biyomedikal Mühendisliği Ana Bilim Dalı, 03030, Afyonkarahisar, ORCID No : <https://orcid.org/0000-0003-0356-017X>**Keywords:**

Biomimetics,
Denativ Hartenberg Method,
Hippotherapy,
Robot Kinematics

Abstract: The engineering perspective on the physiology and anatomy of living things has led to the emergence of the science of biomechanics. Developing computer technologies have made it possible to examine the behaviour of living things in more detail and to develop technologies that enable kinetic and kinematic analysis of movements to imitate real limbs. In this study, the natural gaits of horses (Walk, Canter and Trot) were analysed with image processing techniques, kinematic analyses were made and three-dimensional solid models were created. Giving movement ability to the extracted solid models was carried out with the simulation software prepared on the Matlab-SimMechanic platform. By comparing the findings obtained as a result of image processing and simulation, the success of transferring the movements to a developed system was evaluated. After mathematical equations were created in the MATLAB environment, the equations were tested on the developed system and their performance rates were determined. With the developed system, joint angles, ability to reach the correct position and movement ability were analysed and it was shown how the mathematical equations required to perform the movements could be derived. As a result, a design process model for movement analysis, simulation and control of different living groups is presented with the equations obtained by formulating the information obtained from the developed system.

(Araştırma Makalesi)**Hipoterapi İçin Kinematik Analize Dayalı 3 Boyutlu Modelleme Ve Simülasyon****Anahtar Kelimeler:**

Biyomimetik,
Denativ Hartenberg Yöntemi,
Hipoterapi,
Robot Kinematığı

Özet: Canlıların fizyolojisine ve anatomisine olan mühendislik bakış açısı biyomekanik biliminin ortaya çıkmasını sağlamıştır. Gelişen bilgisayar teknolojileri, canlıların davranışlarını daha detaylı incelemeye, hareketlerin kinetik ve kinematik analizlerini yaparak gerçek uzuvları taklit etmeyi sağlayan teknolojilerin geliştirilmesine olanak sağlamıştır. Bu çalışmada atların doğal yürüyüşleri (Normal, Kenter ve Tırs) görüntü işleme teknikleri ile analiz edilerek kinematik analizleri yapılmış ve üç boyutlu katı modelleri çıkartılmıştır. Çıkarılan katı modellere hareket yeteneğinin kazandırılması Matlab-SimMechanic platformunda hazırlanmış olan simülasyon yazılımı ile gerçekleştirilmiştir. Görüntü işleme ve simülasyon sonucunda elde edilen bulgular kıyaslanarak hareketlerin geliştirilen bir sisteme aktarma başarımı değerlendirilmiştir. Matlab ortamında matematiksel denklemler çıkarıldıktan sonra denklemler geliştirilen sistem üzerinde denenmiş ve başarı oranları tespit edilmiştir. Geliştirilen sistem ile eklem açıları, doğru konuma ulaşma becerileri ve hareket yapabilme yeteneğini analiz edilmiş olup hareketlerin gerçekleştirilmesi için gereken matematiksel denklemlerin nasıl çıkarılabileceği gösterilmiştir. Sonuç olarak, geliştirilen sistemden edinen bilgiler formülize edilerek elde edilen denklemler ile farklı canlı gruplarının hareket analizi, simülasyonu ve kontrolü için bir tasarım süreci modeli sunulmuştur.

1. INTRODUCTION

Scientific analysis of the movements of living things on the 3-dimensional (3D) universe was initiated by Giovanni Alfonso Borelli between 1608 and 1679 [1]. Between 1830 and 1904, Eadweard Muybridge took sequential photographs of a movement, increasing the interest in research on the movements of living things. Northeastern University, developed the first biomimetic robot, a lobster, in 1970, and programmed a library of actions that gave the robotic lobster similar behaviour to real ones [2]. After these first studies, many biomimetic robots that entered the literature were designed and started to be used. These robots are used to perform multiple tasks in diverse fields including the field of biomedical such as diagnosis, surgery, emergency rescue, etc. As an example of its use in the health field, it can be given as a sensory and motor input therapy method to individuals with physical and/or mental problems such as autism by mimicking the characteristic movements of horses [3].

Baniqued and his friends designed a 5-degree-of-freedom robotic exoskeleton for upper extremity treatment using the biomimetic approach. The design of the robotic connections was inspired by the natural morphology of the spongy and cortical bones and their ability to respond to mechanical stress [4]. Solid modelling of the design was carried out in the CAD program CATIA. The use of a biomimetic approach in the design and development of the robotic exoskeleton for rehabilitation holds great promise in promoting the safety and biocompatibility of the device. Ziegler focused on motion synthesis based on 3D motion capture data so that robotic systems used in hippotherapy could create realistic trajectories [5]. A marker selection approach has been developed to extract data describing the rigid body motion of the horseback. The Fourier series method is used to create smooth, cyclic and realistic trajectories, in which the position and direction components of the motion are determined by the least squares point matching algorithm and can be executed effectively by robotic systems. In 2021 Top, inspired by the anatomical features of armido and rosary beetles, developed a functional walker for individuals with orthopaedic disorders. The developed walker, having the anatomical features of the inspired creatures, has the ability to be folded at different angles and also provides individuals with the opportunity to make different postures and sitting positions during walking. The 3D model of the developed walker was created in the CAD environment. Ergonomic risk analysis of the design was carried out with Digital Human Modelling (DHM) using Rapid Upper Extremity Assessment (RULA- Rapid Upper Limb Assessment) and Rapid Entire Body Assessment (REBA) tools of the CATIA V5 program [6]. Trusaji and his friends designed a horse-riding simulator to replicate human gait for hippotherapy in cerebral palsy rehabilitation. In the study, they stated that most of the mechanical horse simulators were designed as an exercise device, not as a rehabilitation device [7].

Literature reviews show that modelling, simulation, and analysis of solid models can be performed in computer

aided environments. For the biomimetic analysis of the developed solid models, the Matlab-SimMechanics tool is preferred in the literature and is used for the control of the systems. Imaging tools (High-speed camera, Kinect sensor, etc.) and different image processing algorithms are used to evaluate the performance of the developed systems. However, the performance rates of biomimetic analyses are not given in those studies, and they are not specified in the mathematical equations. In this study, 3D solid models were created in Solidworks environment after performing kinematic analyses of horses' natural gait types such as Walk gait, Canter and Trot gaits, using image processing techniques in Kinovea environment. Gaining the motion capability to the extracted solid models was carried out with the simulation software prepared on the Matlab-SimMechanic platform. By comparing the findings obtained as a result of image processing and simulation, the performance of transferring movements to a developed system was evaluated. With the developed system, joint angles, ability to reach the right position, and ability to move were analysed and it was shown how the mathematical equations needed to perform the movements could be derived.

2. MATERIALS AND METHODS

The American Robotics Institute defines a robot as a "multifunctional and programmable manipulator designed to move materials, parts and tools, or a special tool that can perform variable programmed movements to perform different tasks". Developing hardware components such as high-speed camera, high-torque actuator, analog and digital converters have increased the mobility of robotic systems. In this way, it has become possible to be used in many areas such as space, military, medical, search and rescue, service sector and home applications [8,9]. With the developments in hardware components, the developments in control algorithms and methods in embedded system software have led to the research of robotic systems, development and the creation of different application examples [10]. Robotic systems are categorized based on various factors that encompass their joint structures, specialized functions, operational principles, application domains, and control methods. In the realm of industrial robotics, classification is based on the functional features they possess and the number of joints they employ. Meanwhile, mobile robots undergo categorization based on the specific areas in which they are deployed and the mechanisms they employ for their operations. Fixed robots are divided into categories like Cartesian robots, cylindrical robots, and more, based on how their parts move. Mobile robots, on the other hand, are split into categories like humanoid, swarm (biomimetic), micro/nano, bio-inspired and collaborative robots depending on their shapes and functions [11].

2.1. Kinematics

Kinematics is the science that studies the structure and movements of a system. The position, acceleration and velocity parameters of the motion are examined using

kinematics. Relationships in kinematic analysis are defined between the end function and the joint angles. Kinematic analyses are divided into two as forward and reverse kinematics [12,13]. Forward kinematics aims to find the position and orientation of the end functionalist with the help of the joint variables (angles) of the robot. It consists of serial limbs connected to each other by prismatic or rotational joints, from a robot body to its end functional. In forward direction kinematics, the position and orientation of the terminal operator is calculated relative to the main frame by giving the joint variables. The relationship between the two limbs is explained by the homogeneous transformation matrix. By using transformation matrices in consecutive joints, the relationship between the base and the end function is defined. Different kinematic methods have been developed to determine the joint variables of robots. These methods can be cited as: homogeneous transformation, Denavit-Hartenberg, Pieper-Roth, zero reference and exponential methods. The Denavit-Hartenberg method is the most preferred method in the literature because it offers a simple and systematic approach for forward and inverse kinematics calculations [14].

2.2 Denavit-Hartenberg Method

The Denavit-Hartenberg Method, which is the most preferred while producing the kinematic model of robots, stands out with its homogeneous transformation matrix (Figure 1). In this method, robot kinematics is determined using four main variables.

$${}_{i-1}T_i = \begin{bmatrix} c\theta_i & -s\theta_i & 0 & a_{i-1} \\ s\theta_i c\alpha_{i-1} & c\theta_i c\alpha_{i-1} & -s\alpha_{i-1} & -s\alpha_{i-1}d_i \\ s\theta_i s\alpha_{i-1} & c\theta_i s\alpha_{i-1} & c\alpha_{i-1} & c\alpha_{i-1}d_i \\ 0 & 0 & 0 & 1 \end{bmatrix}$$

Figure 1. General homogeneous matrix [6].

These variables are:

- a_{i-1} , distance between Z_{i-1} and Z_i
- α_{i-1} , axis angle between Z_{i-1} and Z_i
- d_i is the distance Z_i between X_{i-1} and X_i
- θ_i is the axis angle between X_{i-1} and X_i and Z_i

The above-mentioned main variables are called DH variables. The variables belonging to each addition to the DH table in Table1 are substituted in the general matrix and the transformation matrices are found. The transformation matrix between the main starting point and the end functional position of the robot is obtained by multiplying the transformation matrices of each joint.

Table 1. DH table.

Joint	Alpha	Joint length	Offset Angle	Joint Angle	Joint Variable
i	α_{i-1}	a_{i-1}	d_i	θ_i	θ_i / d_i
1	0	0	0	θ_1	θ_1
2	0	L1	0	θ_2	θ_2
3	0	L2	0	0	0

In order to make kinematic calculations, coordinate systems must be added to the joints of the robot arm as shown in Figure 3 [12].

- First, the sliding directions or the rotation of the joint axes are determined.
- The direction of rotation for rotary axes and the sliding direction for prismatic joints are defined as the Z axis.
- The bond length perpendicular to the Z axis is defined as the X axis.
- After the X and Z axes are determined, the Y axis is determined according to the right-hand rule.
- In the right-hand rule, the thumb indicates the Z axis, the index finger the X axis and the middle finger the Y axis [13,14].

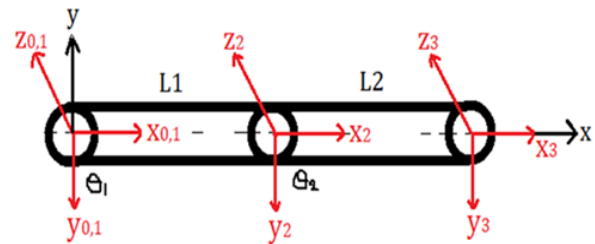


Figure 2. Placing coordinates on joints.

2.2.1 Calculation of Forward Kinematics

The position of the robot's end- effectors, referred to as point P, in Figure 4, can be determined through the utilization of geometric operations and the application of the Denavit-Hartenberg Method, as depicted in Figure 5 and Figure 6. X and Y coordinates can be calculated with the equations given in Equation 1 and Equation 2 .

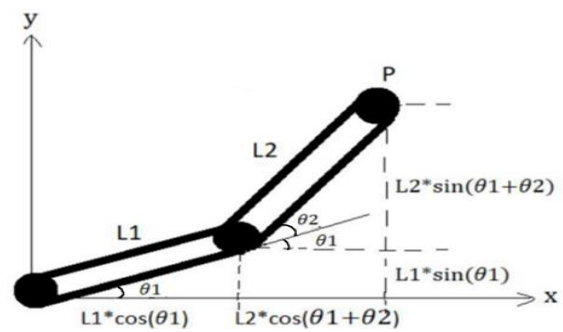


Figure 3. Two-dimensional representation of the robot arm

$${}_{01}T = \begin{bmatrix} \cos(\theta_1) & -\sin(\theta_1) & 0 & 0 \\ \sin(\theta_1) & \cos(\theta_1) & 0 & 0 \\ 0 & 0 & 1 & 0 \\ 0 & 0 & 0 & 1 \end{bmatrix} \quad {}_{12}T = \begin{bmatrix} \cos(\theta_2) & -\sin(\theta_2) & 0 & L1 \\ \sin(\theta_2) & \cos(\theta_2) & 0 & 0 \\ 0 & 0 & 1 & 0 \\ 0 & 0 & 0 & 1 \end{bmatrix}$$

$${}_{23}T = \begin{bmatrix} \cos(\theta_2) & -\sin(\theta_2) & 0 & L1 \\ \sin(\theta_2) & \cos(\theta_2) & 0 & 0 \\ 0 & 0 & 1 & 0 \\ 0 & 0 & 0 & 1 \end{bmatrix}$$

Figure 4. Advanced kinematic computation of the end effector with the Denavit-Hartenberg method

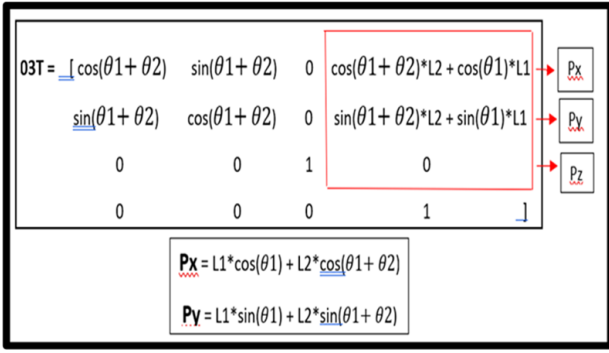


Figure 5. Advanced kinematics calculation of end effector - with Denavit-Hartenberg method

$$Px = L1 * \cos(\theta1) + L2 * \cos(\theta1 + \theta2)^2 \quad (1)$$

$$Py = L1 * \sin(\theta1) + L2 * \sin(\theta1 + \theta2)^2 \quad (2)$$

2.2.2 Calculation of Inverse Kinematics

The inverse kinematics of the robot (Figure 7) aims to reach the joint variables (angles) that the robot should have in cases where the position and orientation of the end point of the robot arm are known. In robotics, inverse kinematics uses kinematic equations to determine the joint parameters that provide the desired position for each of the robot's end-effectors. A good trajectory planning enables the robot to reach the right point with minimum requirements with optimum movements [14,15].

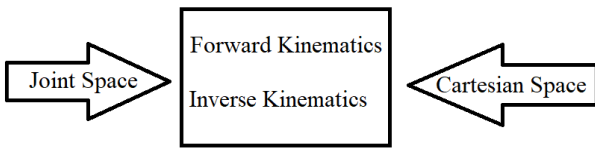


Figure 6. Inverse kinematics analysis [12].

The trigonometric equations used in performing the inverse kinematics solution are given in the equations between Equation 3 and Equation 8.

$$\cos\theta = a \text{ ise } \theta = \arctan2(\pm\sqrt{1 - a^2}, a) \quad (3)$$

$$\sin\theta = a \text{ ise } \theta = \arctan2(a, \pm(\sqrt{1 - a^2})) \quad (4)$$

$$\cos\theta = a \text{ ve } \sin\theta = b \text{ ise } \theta = \arctan2(b, a) \quad (5)$$

$$a\sin\theta + b\cos\theta = 0 \text{ ise } \theta = \arctan2(-b, a) \text{ or } \arctan2(b, -a) \quad (6)$$

$$a\sin\theta + b\cos\theta = c \text{ ise } \theta = \arctan2(a, b) \pm \arctan2(\sqrt{a^2 + b^2 - c^2}, c) \quad (7)$$

$$\sin(\theta1 + \theta2) = \sin\theta1 * \cos\theta2 + \cos\theta1 * \sin\theta2 \quad (8)$$

2.3 Image-Based Motion Analysis

Image-based motion analysis makes it possible to examine a motion within a certain time frame relative to the reference plane. Image recording not only makes it possible to view the motion being examined in the desired time, but also allows freezing of image frames, slow motion, and facilitates analysis [16]. Image-based motion

analysis has become indispensable for the evaluation of motion in the 3D universe. Motion analysis is available in different package programs. Examples of these programs are Kinovea, V1 Home, PhysMo, Tracker, Motion Analysis Tools, Yessoft Sport Video Player and Sports Video Analysis [17]. In this study, the Kinovea software program was preferred for motion analysis. This program is designed to capture, compare, slow down, measure, and compare desired parameters and performances.

2.4 Computer Aided Solid Modelling

Solidworks is a computer-aided engineering (CAE) design program that allows the creation of solid models. This software includes a range of features such as solid part modeling, simulation, motion, assembly, toolbox, tool analyst, e-drawings, Photoview 360, ScanTo3D, and DWG editor [18]. The main advantages of this program to users can be listed as follows:

- In addition to having a simple interface, advanced modeling can be done.
- Analysis, simulation and animation can be done on the designed solid model.
- It is possible to design and assemble machine parts with many sub-components.
- It provides the opportunity to improve their visuals by coloring their designs.
- Design files can be run in analysis programs such as ANSYS.

2.4.1 Matlab –SimMechanic

It is a package program that works in SimMechanics Simulink environment, which provides 3D modelling of mechanical systems. The 3D representation of the models created with this package program can be seen and movements can be monitored during simultaneous simulation. Since SimMechanics works under Simulink, it provides an integrated use of all the possibilities of MATLAB and Simulink software. It is possible to control the mechanical system designed with SimMechanics by combining it with electrical, pneumatic and hydraulic models thanks to Simulink [18].

2.5 3D Modelling Simulation and Application System Based on Kinematic Analysis

The block diagram of the simulation of the implemented system is given in Figure 8. After the images of the living thing were taken from the database, each section was analysed in the Kinovea medium and the data on the joint angles were extracted. Following the completion of the kinematic analysis of the creature's solid model, which was designed within the Solidworks environment, mechanical block diagrams corresponding to the model were generated in alignment with MATLAB SimMechanics. The motion capability of the solid model was simulated by calculating the forward and inverse kinematics of the system in MATLAB's Simulink and GUI environments. The accuracy of the simulation system was determined by transferring the kinematic information obtained as a result of the simulation to the box plot.

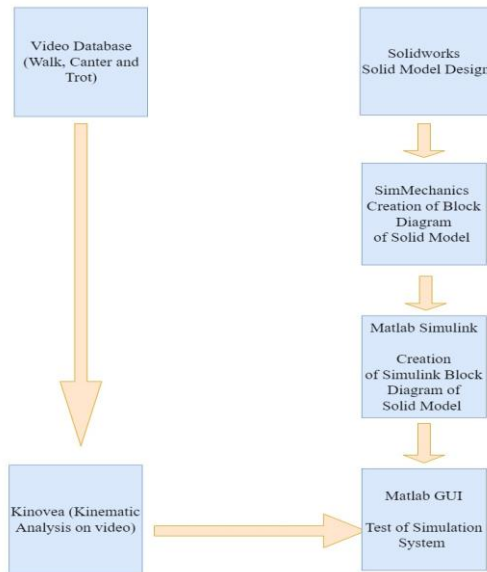


Figure 7. Block diagram of the simulation system

In Figure 8, the block diagram of the application system is given. The real model of the solid model designed in the Solidworks environment was produced with a 3D printer. Then, using the kinematic information obtained as a result of the Kinovea analysis, the conversion equation to the PWM signal was derived by using the curve fitting method. The extracted equations were converted to PWM signals according to the angle information via microcontroller (Atmega 238) and tested on the real system using Futaba S3003 servo motor with the help of PCA9685 servo motor driver. The image recording of the system was taken to analyse the test data. The kinematic analysis of the captured images was carried out in Kinovea environment. The information obtained from the kinematic analysis was transferred to the box graph and the motion capability of the solid model was compared with the real, live motion.

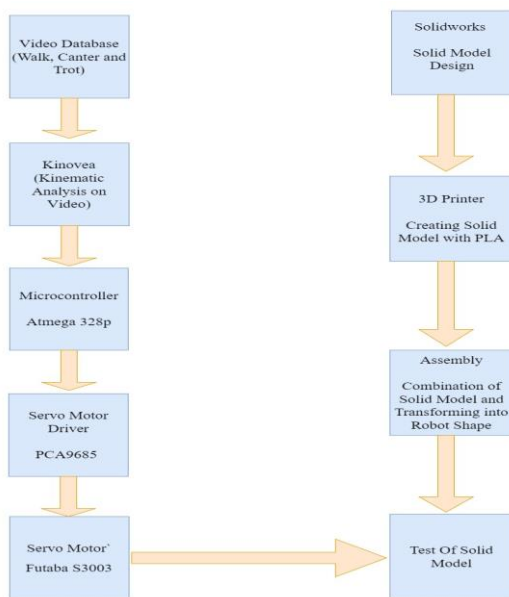


Figure 8. Block diagram of the application system
2.5.1 Performance Test of the System

The flow diagram of the performance test of the system is depicted in Figure 10. Once the images were extracted from the database, a motion analysis was conducted within the Kinovea environment, leading to the acquisition of kinematic data. The acquired information was tested in the developed system. Subsequently, image recordings of the system were captured, and kinematic analysis was executed within the Kinovea environment. The results obtained from the simulation and application system and the actual motion information were transferred to the box graph and the success rate of the developed system was determined.

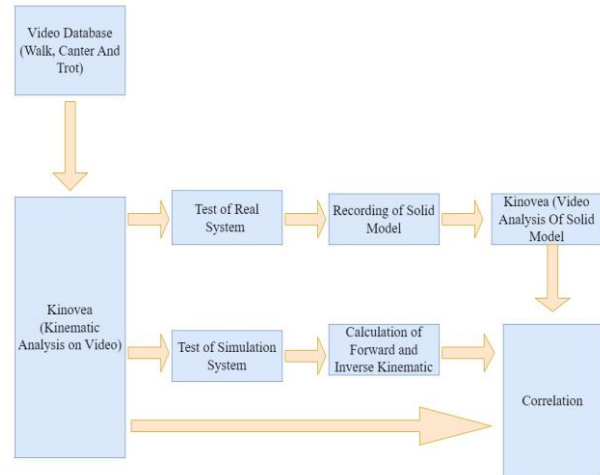


Figure 9. Performance test flowchart

3. RESULTS

In this study, the following findings are presented: the kinematic analysis of live images conducted within the Kinovea environment, the development of a solid model within the Solidworks environment, the simulation of the solid model and subsequent system testing, the creation of an application system, the kinematic analysis of images acquired through the application system, and the exploration of relationships between the simulation system and the application system for the living organism.

3.1 Kinematic Analysis on Live Image in Kinovea Environment

Within the scope of the study, images of Walk gait, Canter gait and Trot gait, which are natural gaits of horses, were taken from the “Horse and Us” blog site [19]. Angle information were obtained using the protractor tool in Kinovea by determining the reference point of the arms (θ_1) and knee (θ_2) on the front legs of the horse, and the hip (θ_1) and knee (θ_2) sections on the hind legs of the horse in the Kinovea environment. The time-varying angle information during Walk gait, Canter gait and trot gait are given in Figure 11. The analysis revealed that both the walk and trot gaits exhibited symmetry, meaning that the movements observed on one side were consistently mirrored on the other side. In contrast, the Canter gait exhibited asymmetrical behaviour, indicating that the movements on the right and left sides were distinct from each other.

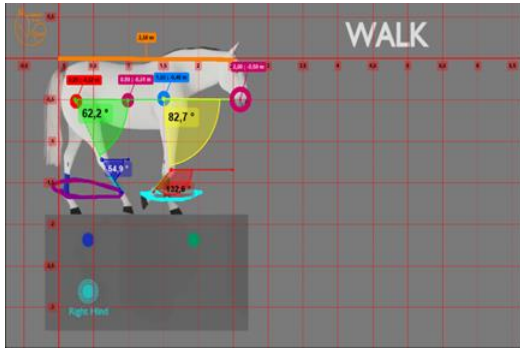


Figure 11a. Reference point and protractor display

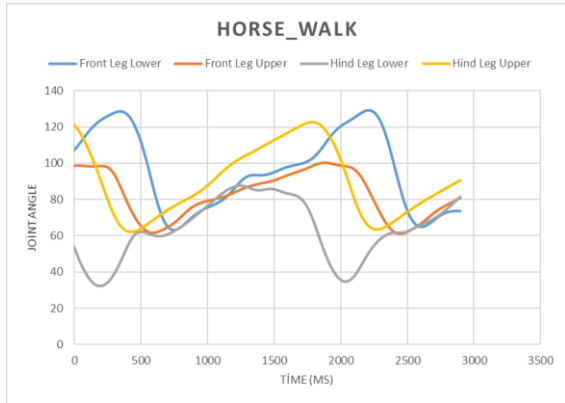


Figure 11b. Walk

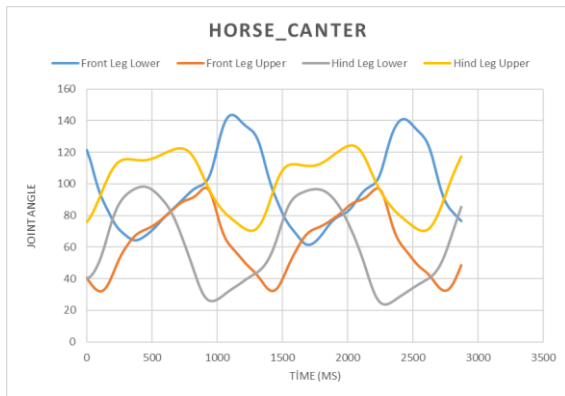


Figure 11c. Canter

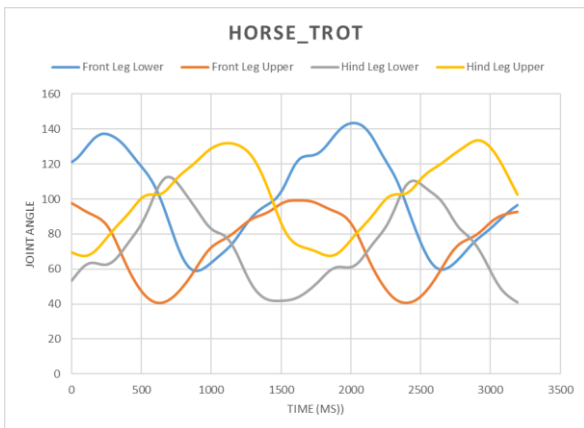


Figure 11d. Trot

Figure 11. Kinematic analysis of the walk, Canter and Trot gait of the living organism in the Kinovea environment.

3.2 Solid Model Design and Simulation

The legs of the solid model (Figure 12a) are designed as humanoids. The legs are aligned side by side and mounted on a flat plate-shaped body. The designed model is 290 cm wide, 46 cm long and 15 cm high. After the solid model was designed in the Solidworks environment, the Simulink model of the model (Figure 12b) was created using the MATLAB SimMechanics plugin.

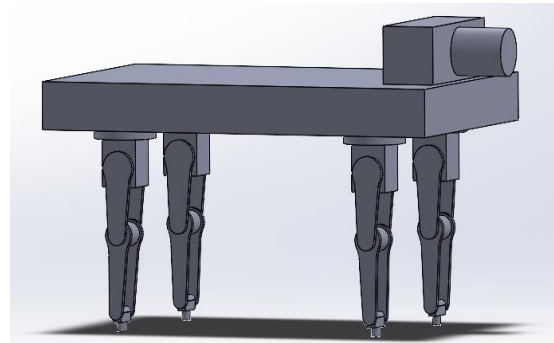


Figure 12a. Solid model design

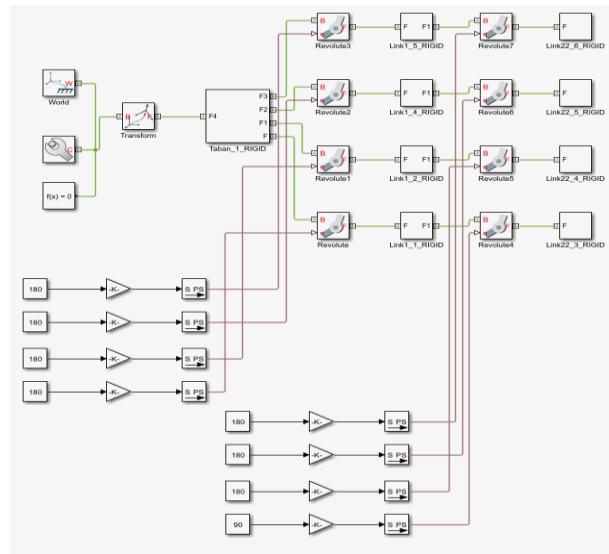


Figure 12b. Simulink model

Figure 12. Solid model design and simulink block diagram

In order to test the kinematic results of the extracted Simulink model in the solid model, the MATLAB GUI interface given in Figure 13 was developed. The program's interface features six buttons. Clicking the "start" button loads and initiates the Simulink model, while clicking the "stop" button halts the Simulink model. If the "Default" button is pressed, all legs of the solid model are automatically maintained in an upright position.

Pressing the Canter, Walk, or Trot buttons performs the calculation of position information using advanced kinematic equations (Equation 4.1 and Equation 4.2). These equations utilize kinematic data previously extracted from the Kinovea analysis and processed through the Denavit-Hartenberg method. The acquired position information was input into Equation 9 until

Equation 16, which represent one of the inverse kinematics equations.

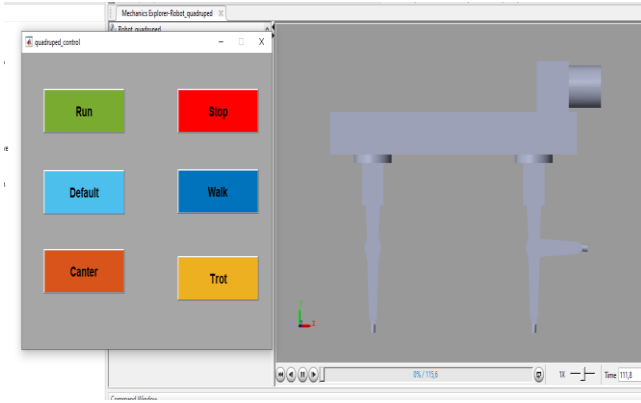


Figure 13. Simulation software

This input yielded angle information, resulting in the emergence of four distinct solution spaces from Equation 9 and Equation 16, which are:

First Solution Space:

$$\theta_2 = \arctan2\left(\sqrt{1 - \frac{px^2 + py^2 - (a2^2 + a1^2)}{2 * a1 * a2}}, \frac{px^2 + py^2 - (a2^2 + a1^2)}{2 * a1 * a2}\right) \quad (9)$$

$$\theta_1 = \arctan2(px, py) + \arctan2(\sqrt{px^2 + py^2 - (a2 * \cos\theta_2 + a1^2)^2}, a2 * \cos\theta_2 + a1) \quad (10)$$

Second Solution Space

$$\theta_2 = \arctan2\left(-\sqrt{1 - \frac{px^2 + py^2 - (a2^2 + a1^2)}{2 * a1 * a2}}, \frac{px^2 + py^2 - (a2^2 + a1^2)}{2 * a1 * a2}\right) \quad (11)$$

$$\theta_1 = \arctan2(px, py) + \arctan2(\sqrt{px^2 + py^2 - (a2 * \cos\theta_2 + a1^2)^2}, a2 * \cos\theta_2 + a1) \quad (12)$$

Third Solution Space

$$\theta_2 = \arctan2\left(\sqrt{1 - \frac{px^2 + py^2 - (a2^2 + a1^2)}{2 * a1 * a2}}, \frac{px^2 + py^2 - (a2^2 + a1^2)}{2 * a1 * a2}\right) \quad (13)$$

$$\theta_1 = \arctan2(px, py) - \arctan2(\sqrt{px^2 + py^2 - (a2 * \cos\theta_2 + a1^2)^2}, a2 * \cos\theta_2 + a1) \quad (14)$$

Fourth Solution Space

$$\theta_2 = \arctan2\left(-\sqrt{1 - \frac{px^2 + py^2 - (a2^2 + a1^2)}{2 * a1 * a2}}, \frac{px^2 + py^2 - (a2^2 + a1^2)}{2 * a1 * a2}\right) \quad (15)$$

$$\theta_1 = \arctan2(px, py) - \arctan2(\sqrt{px^2 + py^2 - (a2 * \cos\theta_2 + a1^2)^2}, a2 * \cos\theta_2 + a1) \quad (16)$$

It has been determined that the equations belonging to the third solution space from the solution spaces given above gave correct results. As a result of inverse kinematics equations, the correct solution spaces of inverse kinematics were determined by calculating the Euclidean distance between the angle information obtained from the Kinovea analysis and the position information of the newly calculated angle information. According to the simulation results, in the first, second and fourth solution spaces, the lower and upper joint angles (THETA1 and THETA2) showed opposite relationships from each other, while in the third solution space, both lower joint angles and upper joint angles showed a linear relationship. Therefore, in this study, the third solution space was determined as the most successful solution space among the solution spaces.

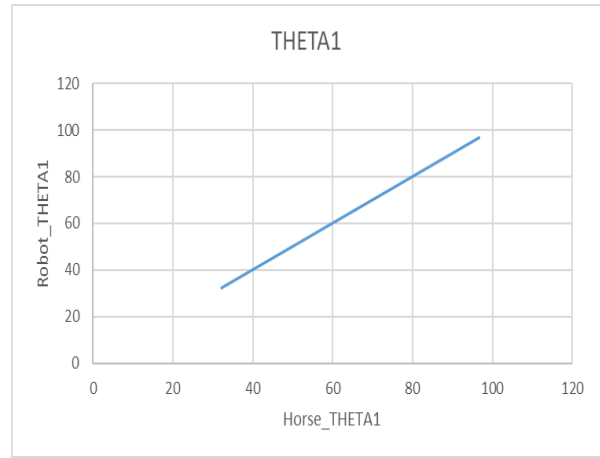


Figure 14a. Upper joint angle

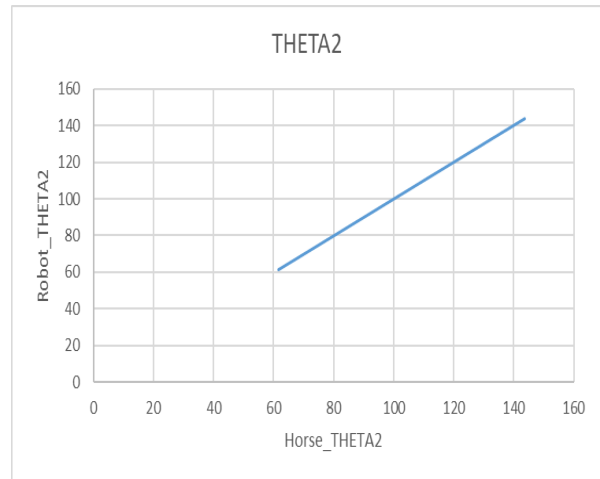


Figure 14b. Lower joint angle

Figure 14. simulation results of third solution space

3.3 Creation of the Application System

After the solid model was designed in Solidworks environment, STL files were extracted, and parts were produced using PLA material from a 3D printer. The solid model created has a width of 46 cm, a length of 29 cm and a height of 36 cm. The humanoid legs of the solid model are formed by combining the produced parts with Futaba S3003 servo motors that act as joints, as seen in Figure 15.

Equations for controlling servo motors are given to Atmega 328 microcontroller. The PWM signal of the servo motors is set at 400 micro seconds (0 degrees), 1.2 milliseconds (90 degrees), and 2 milliseconds (180 degrees).

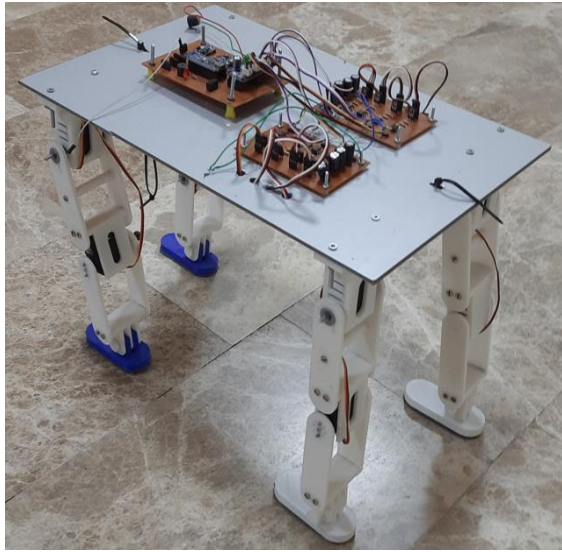


Figure 15. Implemented application system.

The kinematic information (angle) is adjusted to the PWM signal with the help of curve fitting method. As a result of the curve fitting method, two equations were obtained according to the mounting directions of the servo motors. These are given in Equation 17 and Equation 18 as m1 and m2.

$$m1 = (8.8889 * \theta) + 400 \quad (17)$$

$$m2 = 2000 - (8.8889 * \theta) \quad (18)$$

3.4 Comparison of Simulation System and Real System

The kinematic analysis (Figure 16) was carried out by using the method applied in the analysis of the living organism in the Kinovea medium, also in the solid model. Kinematic analysis was performed separately for each of the walk, canter and trot gaits.

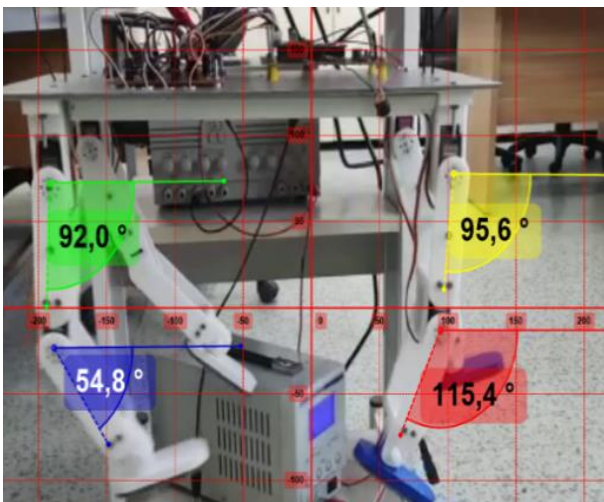


Figure 16a. Reference point and protractor display

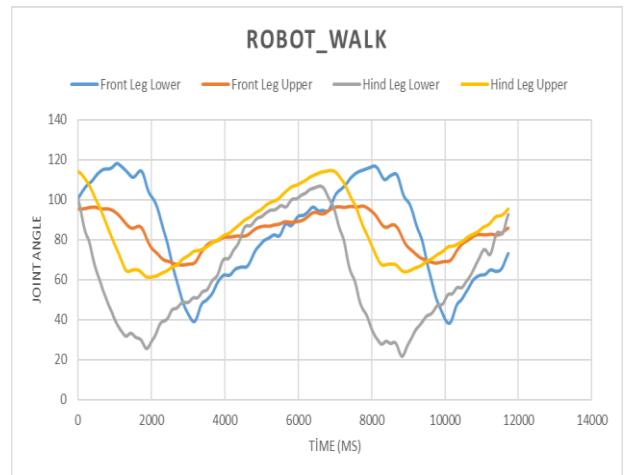


Figure 16b. Joint angle change over time

Figure 16. Kinematic analysis of the walk gait of the solid model in the Kinovea environment.

The correlation relations between the real images of the horse and the system realized are given in Table 2. Upon examining the correlation table presented in Table 2, it is evident that the gait model exhibiting the lowest average correlation is the walk gait, whereas the highest correlation among the gait models was observed in the trot gait.

Table 2. Correlation between different walking patterns of solid model (Robot)

Joint	Walk	Canter	Trot	Overall average of joints
Front Leg Lower	0.9013	0.8901	0.8310	0.8741
Front Leg Upper	0.9463	0.9400	0.9891	0.9584
Hind Leg Lower	0.7700	0.8143	0.8746	0.8196
Hind Leg Upper	0.9279	0.9807	0.9411	0.9499
Overall Average of Gaits	0.8863	0.9062	0.9089	

In each gait model, it is seen that the least correlation relationship is in the lower joints and the most correlation relationship is in the upper joints. The reason for this might be due to the fact that the upper joints are connected to the body and the lower joints are connected to the body in a distant position. Moreover, because the solid model is made with PLA material and depending on the continuous movement, deformation occurs at the joint points of the material.

4. DISCUSSION AND CONCLUSION

In this study, it is aimed to develop a system that allows the testing of biomimetic systems, which are costly in design and construction, before they are physically implemented. Within the scope of the study, the natural gaits of horses (Walk, Canter and Trot) whose anatomy is similar to human anatomy were determined in Kinovea environment and 3D solid models were created in Solidworks environment. Gaining mobility to the

extracted solid models is provided by the simulation interface software prepared on the Matlab-SimMechanics platform. By comparing the findings obtained as a result of image processing and simulation, the performance of transferring movements to a developed system was evaluated.

In the studies in the literature, it is seen that computer aided environments are used for modeling, simulation and analysis of solid models. Matlab-SimMechanics tool was also preferred in the literature for biomimetic analysis of the developed solid models and kinematic analyzes were made to control the systems. Image analysis method was used to evaluate the performance of the developed systems. Nevertheless, these studies do not provide performance metrics for biomimetic analyses, nor do they present the mathematical equations employed for these analyses. The equations used in the analysis are given together with their coefficients in Appendix A. A review of the literature in this domain reveals that there is a gap in this regard.

In this study, the mathematical equations of biomimetic analyzes were calculated in Matlab, tested in a real system, and the success rates were calculated. With the developed system, joint angles, ability to reach the right position and ability to move were analyzed and it was shown how to derive the mathematical equations required for the realization of movements. To address this issue, the process involved capturing images of the living organism, which were subsequently input into the database. Following this step, kinematic data was extracted within the Kinovea environment. The correct solution space was determined by transferring the extracted information to the simulation system. Then, the angle equation of the gait models was found by using the Curve Fitting tool, which is one of the Matlab tools for the same kinematic information. As a result, the information obtained from the developed system was formulated and the movement analysis of different living groups.

During the investigation of these analyses, several problems were encountered that affected the performance rate of the system. One of the biggest challenges in the simulation was the accurate transfer of the kinematic data extracted from Kinovea into the simulation environment. Inaccuracies in calibration and noise in the data complicated this process and required careful fitting and validation procedures.

One of these problems was that the motor drivers available on the market did not have the required resolution. This affected the stable operation of the control system, as the operating voltage range of the motors used in the system and the currents they drew caused disturbances in the system. The study concluded that to solve this problem, optical isolation should be used between the control unit and the motor drivers. In addition, since the construction of the system was made of PLA material, the stiffness of the system was lost due to deformation over time. Some improvements are suggested below that could make the system work better in future studies:

- Since the resolution of the system's motor driver is important, high-resolution motor driver circuits should be designed or used.
- The construction material should be made of a lighter material, such as aluminium, so that it is stiff and stable and is not deformed by the friction that occurs during motion.
- A high torque must be selected so that the joints of the system move more rhythmically and are balanced.

the expected effects of using high-resolution motor drivers and lighter construction materials on the overall stability and performance of the biomimetic system are as follows:

High resolution motor drivers:

Improved precision: High-resolution motor drivers offer finer control over the movement of the system's components. This precision is particularly important in biomimetic systems where it is important to accurately mimic natural movements.

Smooth movement: With higher resolution, the system can perform smoother movements, reducing jerky movements that could affect stability or accuracy.

Better responsiveness: The system can react faster to commands or changes in environmental conditions, allowing for real-time adjustments and better interaction with the environment.

Reduced vibration: Higher resolution can mitigate vibrations that may occur during movement, which is especially important for delicate tasks or when interacting with sensitive environments or organisms.

Lighter construction materials (e.g. aluminum):

Increased agility: Lighter materials reduce the overall weight of the system and improve its agility and maneuverability. This is particularly beneficial for biomimetic systems, which are designed to mimic the agility of natural organisms.

Improved energy efficiency: With less mass to move, the system requires less energy to operate, resulting in improved energy efficiency and potentially longer operating times, especially for battery-powered systems.

Minimized deformation: Lighter materials such as aluminum are less susceptible to deformation due to friction or stress during movement. This helps maintain the structural integrity of the system over time and ensures consistent performance.

Better portability: A lighter system is easier to transport and use in different environments, making it more versatile and adaptable for different applications or research scenarios.

Overall impact:

Increased stability: The combined use of high-resolution motor drivers and lighter construction materials can result in an overall more stable system. The precise control provided by the motors, combined with the structural stability provided by lightweight materials, helps to minimize deviation from intended movements and prevent instability or wobble during operation.

Improved performance: By optimizing both control precision and structural integrity, the biomimetic system can achieve a higher level of performance in terms of accuracy, reliability and adaptability to dynamic conditions. This can be critical in applications such as robotic surgery, prosthetics or environmental monitoring where precision and stability are essential.

In summary, the integration of high-resolution motor drivers and lighter construction materials into a biomimetic system can significantly improve its stability, precision and overall performance, enabling more effective mimicking of natural behaviors and better interaction with the environment.

The developed system can thus be used to study and analyze the behavior of living beings, whether as a hippotherapy simulator or in the field of biomimetics. In order to increase the functionality of the system, bidirectional servomotors or stepper motors with compact design, zero backlash, high dynamics, high torsional and tilting stiffness, small size, low mass, easy installation, high load capacity of the radial-axial output bearing and easy maintenance can be used as an alternative to the servomotor model used in this study. It is therefore expected that the errors that can occur will be reduced and the system can be used in the laboratory environment.

In summary, the developed system offers immense potential for a wide range of applications in various research and therapeutic contexts due to its ability to study and analyze the behavior of living organisms with remarkable precision.

Biomedical research:

The system can be used as a valuable tool in biomedical research, allowing scientists to study and understand the intricacies of animal behavior and physiology. This can help in the development of new treatments and therapies for various medical conditions. By simulating certain animal movements or behaviors, researchers can study biomechanics, neurology and other areas related to human and animal health. For example, studying the gait patterns of animals could contribute to the development of better prostheses or rehabilitation strategies for people with mobility impairments.

Therapeutic applications:

In addition to its applications in research, the system also has considerable potential in therapeutic areas. In hippotherapy, for example, where the movements of horses are used as a therapeutic measure for people with physical or cognitive impairments, the system can serve as a realistic simulator to supplement conventional therapy sessions. In addition, the system can be adapted for use in sensory integration therapy, where precise sensory input is provided to individuals with sensory processing disorders or autism spectrum disorders. By mimicking the movements of different animals, the system can provide customized sensory experiences that promote relaxation, sensory regulation and social interaction.

Educational tools:

The system can also be used as an educational tool in academic institutions and rehabilitation centers. It can provide students and therapists with hands-on experience in understanding animal behavior and its application in therapy and rehabilitation. In addition, the versatility of the system allows for customization and integration into curricula tailored to specific learning objectives, enhancing the learning experience for students and professionals alike.

Robotics and biomimetics:

In addition to therapeutic and research applications, the system can also contribute to advances in robotics and biomimetics. By accurately replicating the movements and behaviors of animals, it can inspire the development of more agile and adaptable robotic systems for tasks such as search and rescue, environmental monitoring and exploration of difficult terrain. To summarize, the developed system represents a versatile platform with broad applications in biomedical research, therapy, education and robotics. The precise control and realistic simulation capabilities make it a valuable tool to advance scientific knowledge, improve therapeutic interventions and stimulate innovation in various fields. As the technology continues to evolve, the potential for further innovation and refinement of the system's capabilities is virtually limitless and promises further contributions to research, therapy and education in the years to come.

Ethical concerns

compliance with ethical rules

This research has shown compliance with the rules determined within the framework of the "Higher Education Institutions Scientific Research and Publication Ethics Directive" at all stages from planning to implementation, from data collection process to data analysis. There has not been any violation of the rules under the title "Actions Contrary to Scientific Research and Publication Ethics", which is the second part of the Directive. Scientific ethics and citation rules were fully followed during the writing process of the study, no manipulation was made on the collected data, and this study was not sent for evaluation in any other academic publication environment.

Finance

The authors declare that they have not received a special grant from funding organizations in the public, commercial or non-profit sectors for this study.

Conflict of interest

As the authors, we confirm that there is no conflict of interest with any person or institution related to this study.

REFERENCES

- [1] <https://www.sci-sport.com/en/theory/chapter-1-history-and-rise-of-biomechanics.php>.

- [2] Ayers, J., Witting, J. (2007). Biomimetic approaches to the control of underwater walking machines. *Philos Trans A Math Phys Eng Sci.*, 15; 365 (1850): 273-95. doi: 10.1098/rsta.2006.1910. PMID: 17148060.
- [3] Koca, T. T., Ataseven, H., (2015). What is hippotherapy? The indications and effectiveness of hippotherapy. *Northern clinics of Istanbul*, 2(3), 247.
- [4] Baniqued, P.D.E., Dungao, J.R., Manguerra, M.V., Manguerra, R.G., Abad, A.C., Bugtai, N.T. (2018). Biomimetics in the Design of a Robotic Exoskeleton for Upper Limb Therapy, *AIP Conference Proceedings*, 1993, 040006.
- [5] Ziegler, J., Gattringer, H., Reiter, A., Hormandinger, P., Müller, A., Mitterhumer, M. (2018). Generation of realistic saddle trajectories from captured horseback motion, *Multibody System Dynamics*, 52, 117-133.
- [6] Top, N., Başak, H., Şahin, İ. (2021). Biyomimetik Tabanlı Fonksiyonel Yürüteç Tasarımı ve Dijital İnsan Modelleme ile Ergonomik Analizi, *El-Cezeri*, 8, 618-634.
- [7] Trusaji, W., Satriawan, A., Rahadini, S. S., Hasanuddin, M.O., Setianingsih, G., Pratomo, N, vd. (2022). Horse Riding Simulator Design to Replicate Human Walking Gait for Hippotherapy in Cerebral Palsy Rehabilitation, *Machines*, 10, 1060.
- [8] Jones, J.L., Flynn, A.M., Seiger, B.A. (1993). *Mobile Robots-Inspiration to Implementation*, AK Peters Ltd. Wellesley, Massachusetts.
- [9] Everett, H. R (1995). *Sensors for Mobile Robots*, CRC Press, 542p, Ney work.
- [10] Gürgüze, G., Türkoğlu, İ. (2019). Robot sistemlerinde kullanılan algoritmalar, *Türk Doğa ve Fen Dergisi*, 8, 17-31.
- [11] Çengelci, B., Çimen, H. (2005). Endüstriyel robotlar, *Makine Teknolojileri Elektronik Dergisi*, 2, 69-78.
- [12] Kyriakopoulos, K.J., Loizou, S. G. (2006). *Robotics: Fundamentals and Prospects*, Çev.: Demircioğlu P, Bögrekci İ, 15s.
- [13] Kuşcu H. (2007). DersNotları Temel Robotik, https://hilmi.kulubevet.com/ders_notlari/robotik/Temel%20Robotik2.pdf (Erişim Tarihi: 03.06.2023).
- [14] Küçük, S., Bingül, Z. (2004). Robot sistemlerinde kinematik yöntemlerin karşılaştırılması, *Politeknik Dergisi*, 7, 107-117.
- [15] Ünver, B. (2005). Artık robot kollarının ters kinematik problemlerinin çözümü ve gerçekleştirilmesi, İstanbul Teknik Üniversitesi, Fen Bilimleri Enstitüsü, Yüksek Lisans Tezi, İstanbul.
- [16] Armand, S., Bonnefoy, A., Sagawa, Y., Turcot, K. (2014). *Analyse Du Mouvement Dans Un Contexte*

Clinique, Manuel pratique de chirurgie orthopédique, 3-33.

- [17] Guzmán-Valdivia, C.H., Blanco-Ortega, A., Oliver-Salazar, M.Y., Carrera-Escobedo, J.L. (2013). Therapeutic motion analysis of lower limbs using Kinovea, *Int J Soft Comput Eng*, 3, 2231-307.
- [18] Vural, A., Çiçekoğlu, B., Tuncer, S. (2020). *Bilgisayarda_Kati_Modelleme*. http://meslek.eba.gov.tr/upload/dk10/Bilgisayarda_Kati_Modelleme_10_29_30.pdf. (Erişim Tarihi: 03.06.2023).
- [19] Maria, 2023. The 4 basic horse gait. <https://www.horsesandus.com/the-4-basic-horse-gaits-explained/> (Erişim Tarihi: 03.06.2023).

Appendices

The equations below were determined as sixth-degree sine functions using curve fitting methods in Matlab, based on the image processing data acquired in the Kinovea environment.

Front Leg Lower :

$$f(x) = a1 * \sin(b1 * x + c1) + a2 * \sin(b2 * x + c2) + a3 * \sin(b3 * x + c3) + a4 * \sin(b4 * x + c4) + a5 * \sin(b5 * x + c5) + a6 * \sin(b6 * x + c6)$$

Coefficients (with 95% confidence bounds):

a1 = 160.7	b1 = 0.002092	c1 = 0.04154
a2 = 106.2	b2 = 0.004170	c2 = 1.65400
a3 = 15.21	b3 = 0.008079	c3 = 1.42600
a4 = 5.281	b4 = 0.016070	c4 = 0.38690
a5 = 57.46	b5 = 0.020030	c5 = 0.94430
a6 = 55.60	b6 = 0.020320	c6 = 3.89200

Front Leg Upper:

$$f(x) = a1 * \sin(b1 * x + c1) + a2 * \sin(b2 * x + c2) + a3 * \sin(b3 * x + c3) + a4 * \sin(b4 * x + c4) + a5 * \sin(b5 * x + c5) + a6 * \sin(b6 * x + c6)$$

Coefficients (with 95% confidence bounds):

a1 = 146.1	b1 = 0.001203	c1 = 1.7170
a2 = 92.95	b2 = 0.002749	c2 = 4.2290
a3 = 6.483	b3 = 0.011640	c3 = 0.4364
a4 = 409.2	b4 = 0.029870	c4 = -0.837
a5 = 1.954	b5 = 0.018910	c5 = 3.5290
a6 = 408.8	b6 = 0.029870	c6 = 2.3020

Hind Leg Lower:

$$f(x) = a1 * \sin(b1 * x + c1) + a2 * \sin(b2 * x + c2) + a3 * \sin(b3 * x + c3) + a4 * \sin(b4 * x + c4) + a5 * \sin(b5 * x + c5) + a6 * \sin(b6 * x + c6)$$

Coefficients (with 95% confidence bounds):

a1 = 103.8	b1 = 0.002182	c1 = -0.1692
a2 = 16.62	b2 = 0.008154	c2 = 1.83600
a3 = 6.674	b3 = 0.012120	c3 = 2.122
a4 = 26.56	b4 = 0.003266	c4 = 1.412
a5 = 2.041	b5 = 0.021950	c5 = 3.598
a6 = 1.268	b6 = 0.019040	c6 = 2.959

Hind Leg Upper1:

$$f(x) = a1 * \sin(b1 * x + c1) + a2 * \sin(b2 * x + c2) + a3 * \sin(b3 * x + c3) + a4 * \sin(b4 * x + c4) + a5 * \sin(b5 * x + c5) + a6 * \sin(b6 * x + c6)$$

Coefficients (with 95% confidence bounds):

a1 = 165.1	b1 = 0.001977	c1 = 0.3713
a2 = 60.64	b2 = 0.003418	c2 = 2.9340
a3 = 9.637	b3 = 0.008457	c3 = 2.2900
a4 = 10.93	b4 = 0.011580	c4 = 2.7030
a5 = 152.4	b5 = 0.022400	c5 = -2.900
a6 = -151.4	b6 = 0.022410	c6 = 3.3680